Contribution from the Institut de Topologie et de Dynamique des Systèmes de l'Université Paris 7, CNRS URA 34, 1 Rue Guy de la Brosse, 75005 Paris, France

Kinetic and Thermodynamic Study of Complex Formation between Iron(II) and Pyridoxal Isonicotinoylhydrazone and Other Synthetic Chelating Agents

Jacques-Emile Dubois, Hussein Fakhrayan, Jean-Pierre Doucet, and Jean-Michel El Hage Chahine*

Received July 2, 1991

In neutral aqueous media pyridoxal isonicotinoylhydrazone (PIH), pyridoxal benzoylhydrazone (PBH), salicylaldehyde isonicotinoylhydrazone (SIH), and salicylaldehyde benzoylhydrazone (SBH), which show interesting potential for iron mobilization in living cells, form bicomplexes with Fe(II) in two kinetically distinguishable steps. The first is fast and is ascribed to complex formation with a single ligand; second-order rate constants are 1.65×10^5, 1.70×10^5, 0.85×10^5, and 0.60×10^5 mol^{-1} dm^3 s^{-1} for PIH, PBH, SIH, and SBH, respectively. Bicomplex formation is slower and occurs for the same ligands with second-order rate constants 2.45×10^4, 3.05×10^4, 4.00×10^4, and 1.50×10^4 mol^{-1} dm^3 s^{-1}. The affinities of the four chelates to Fe(II) are rather high, 7.7×10^9, 12.5×10^9, 0.60×10^9, and 0.25×10^9 mol^{-2} dm^6, but cannot be directly correlated with their abilities to mobilize iron in vivo.

Pyridoxal isonicotinoylhydrazone (PIH), pyridoxal benzoylhydrazone (PBH), salicylaldehyde isonicotinoylhydrazone (SIH), and salicylaldehyde benzoylhydrazone (SIH) (Chart I) were synthesized in order to replace the drug desferrioxamine commonly used for mobilizing iron in the therapy of iron overload.[1-6] Some of these ligands (e.g. PIH and PBH) are more efficient than desferrioxamine in mobilizing nonheme iron from the precursors of red cells.[2,5,6]

A large number of spectroscopic and physicochemical analyses were performed mostly on PIH.[5-8] They showed that two ligands are usually involved in the complex with one Fe(III),[7-9] with an estimated average constant $\log K \sim 8.7$.[5] Moreover, it seems that even if Fe(II) is involved in the complexation process, in the final complex the metal is always in the Fe(III) form.[9] The oxidation of Fe(II) to Fe(III) is probably enhanced by complex formation, as observed with some other ligands such as EDTA, oxalates, phosphates, citrates, etc.[10] In addition, the four compounds of Chart I probably exist as several structures related to the acidity of the medium.[11,12] Each of these can complex iron differently. This associates complex formation and mobilization in vivo with the acidity of the cell compartments in which it occurs. These can be the mildly acidic (pH < 6) vesicles responsible for the transport of the iron-loaded transfer protein transferrin from the plasma membrane to its iron-demanding targets inside the cell.[13,14] Nonheme iron mostly occurs in vivo as Fe(III).[14-17] However,

Chart I

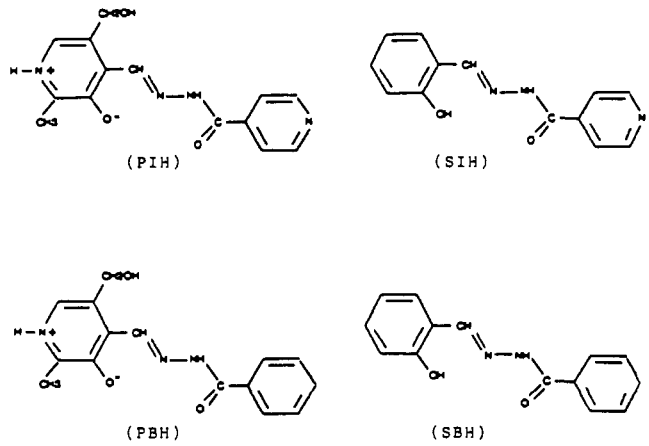

the latter is reduced to Fe(II) by an enzyme (reductase) before its natural mobilization from the transferrin-loaded vesicles.[14] This mobilization process also requires the presence of a reductant such as ascorbate and a Fe(II) cytoplasmic carrier.[14] Moreover, Fe(II) is considered as the form in which iron reacts in vivo with the synthetic chelating ligands of Chart I.[3,16] This can explain the fact that, for example, PIH can mobilize iron from transferrin though the affinity of the latter for Fe(III) is about 10^{12} times greater than that of the chelate (affinity to transferrin is 10^{21} mol^2 dm^{-6} and that to PIH $10^{8.7}$ mol^2 dm^{-6}).[5,14] All these arguments, which confirm the importance of complex formation with Fe(II) in the metabolism of iron, and the lack of any kinetic and thermodynamic knowledge concerning the behavior of the chelating ligands of Chart I with Fe(II) led us to this chemical relaxation[18,19] analysis of complex formation between PIH, PBH, SIH, and SBH with Fe(II).

Experimental Section

PIH, PBH, SIH, and SBH were kindly provided by Professors Schulmann and Ponka from Montréal, Canada. KCl (Merck Suprapur), H_2SO_4 (Prolabo RP), ethanol (Merck), and sodium cacodylate (Aldrich) were used without further purification. $FeSO_4$ (Aldrich Gold-label) was used as received and stored under argon. Water was distilled twice under argon and stored under vacuum.

Stock Solutions. All stock solutions were used fresh and were prepared and handled under argon. $FeSO_4$ solutions (5×10^{-5} to 2×10^{-3} M) were prepared by microinjections of weighed volumes of $FeSO_4$ (0.1 mol dm^{-3}

(1) Ponka, P.; Borova, J.; Neuwirt, J.; Fuchs, O.; Necas, O. *Biochim. Biophys. Acta* **1979**, *586*, 278.
(2) Huang, A. R.; Ponka, P. *Biochim. Biophys. Acta* **1983**, *757*, 306.
(3) Ponka, P.; Schulman, H. M.; Wilczynska, A. *Biochim. Biophys. Acta* **1983**, *718*, 151.
(4) Ponka, P.; Borova, J.; Neuwirt, J.; Fuchs, O. *FEBS. Lett.* **1979**, *97*, 317.
(5) Avramovici-Grisaru, S.; Sarel, S.; Link, G.; Hershko, C. *J. Med. Chem.* **1983**, *26*, 298.
(6) Ponka, P.; Richardson, D.; Baker, E.; Schulman, H. M.; Edward, J. T. *Biochim. Biophys. Acta* **1988**, *967*, 122.
(7) Murphy, T. B.; Johnson, D. K.; Rose, N. J.; Aruffo, A.; Schomaker, V. *Inorg. Chim. Acta* **1982**, *66*, L67.
(8) Aruffo, A.; Murphy, T. B.; Johnson, D. K.; Rose, N. J.; Schomaker, V. *Inorg. Chem. Acta* **1982**, *67*, L25.
(9) Avramovici-Grisaru, S.; Sarel, S.; Cohen, S.; Bauminger, R. E. *Isr. J. Chem.* **1985**, *25*, 288.
(10) Harris, D. C.; Aisen, P. *Biochim. Biophys. Acta* **1973**, *329*, 156.
(11) Metzler, D. E. *Advances in Enzymology*; Meister, E. A., Ed.; Wiley: New York, 1979; Vol. 50, pp 1-37.
(12) Metzler, C. A.; Cahill, A.; Metzler, D. E. *J. Am. Chem. Soc.* **1980**, *102*, 6075.
(13) Thorstense, K.; Romslo, I. *J. Biol. Chem.* **1988**, *263*, 8844.
(14) Nunez, M. T.; Gaete, V.; Abra Watkins, J.; Glass, J. *J. Biol. Chem.* **1990**, *265*, 6688.
(15) Mayer, D. E.; Rohrer, J. S.; Schoeller, D. A.; Harris, D. C. *Biochemistry* **1983**, *22*, 876.
(16) Ponka, P.; Grady, R. W.; Wilczynska, A.; Schulman, H. M. *Biochim. Biophys. Acta* **1984**, *802*, 477.
(17) Theil, E. *Advances in Enzymology*; Meister, E. A., Ed.; Wiley: New York, 1990; Vol. 63, pp 421-448.
(18) (a) Eigen, M.; DeMayer, L. *Techniques of Chemistry*; Weissenberger, A., Hammes, G., Eds.; Wiley: New York, 1973; Part 2, Vol. 6. (b) Bernasconi, C. F. *Relaxation Kinetics*; Academic Press: New York, 1976.
(19) (a) El Hage Chahine, J. M.; Dubois, J. E. *J. Am. Chem. Soc.* **1983**, *108*, 2335. (b) El Hage Chahine, J. M. *J. Chem. Soc., Perkin Trans. 2* **1990**, 505. (c) El Hage Chahine, J. M. *Ibid.* **1990**, 1045.

0020-1669/92/1331-0853$03.00/0

Chart II

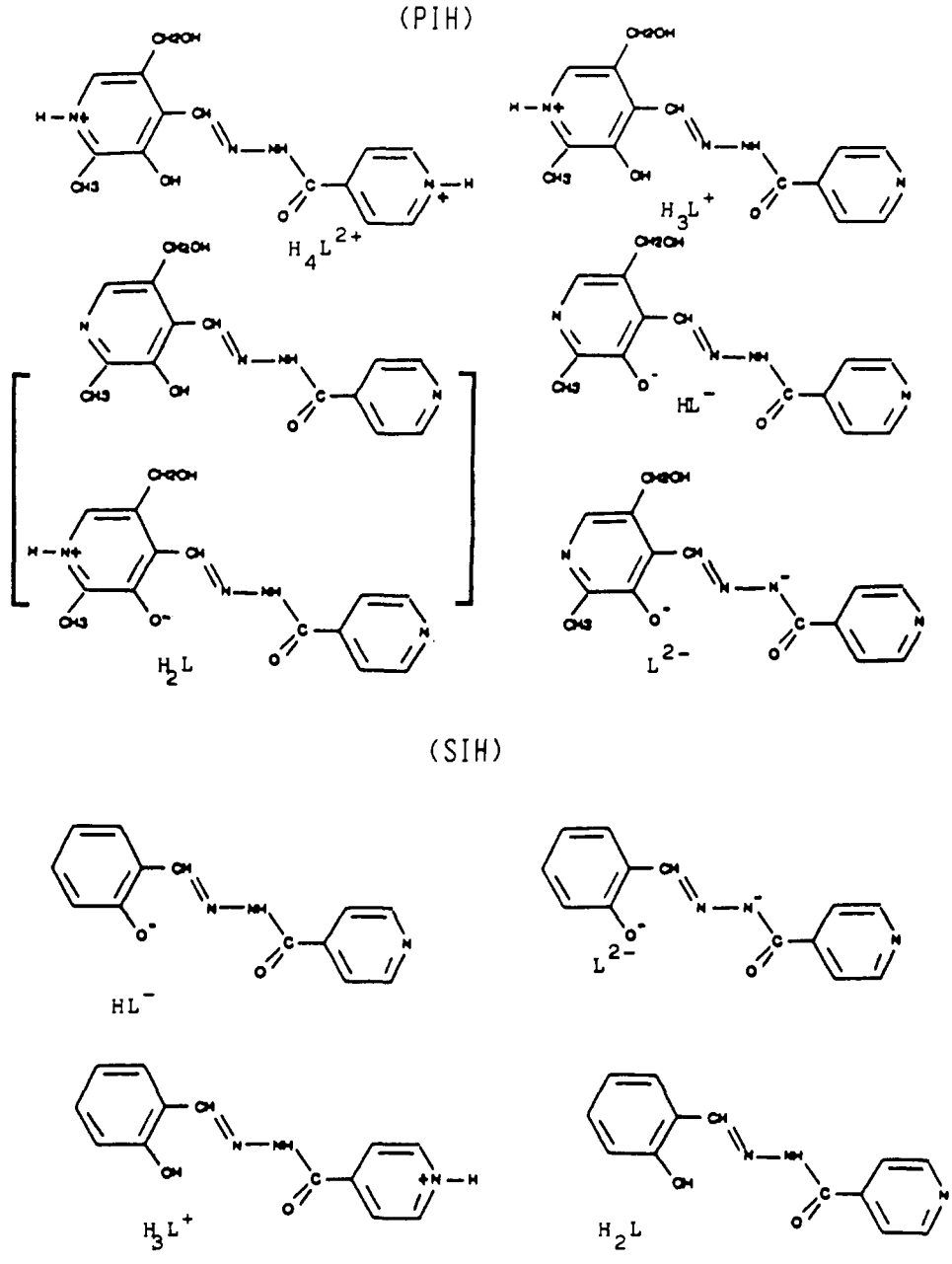

In PBH and SBH the isonicotinoyl is replaced by a benzoyl.

each) in oxygen-free aqueous solutions of 10^{-3} mol dm^{-3} H_2SO_4. PIH and PBH solutions (4×10^{-5} to 5×10^{-4} mol dm^{-3}) were directly prepared in neutral cacodylate (0.01 mol dm^{-3}) buffers, while those of SIH and SBH were obtained by microinjections of concentrated ethanolic solutions into the buffer. The final ionic strength after mixing was adjusted to 0.2 mol dm^{-3} with KCl, and the final pH was 6.86.

pH Measurements. pH values were measured with a Radiometer pH-meter equipped with a "Metrohm E. A. 125" combined electrode. Buffers used for pH standardization were pH 6.86 and 10.01 NBS standards (Beckman).[19]

Spectrophotometric Measurements. Spectrophotometric measurements were performed under nitrogen at 25 ± 0.5 °C on Cary C210 and Varian DMS 200 spectrophotometers both equipped with magnetic stirring devices and thermostated cell carriers.

Stopped-Flow Measurements. Kinetic measurements were performed under argon on a Canterbury High-tech stopped-flow spectrophotometer equipped with a thermostated bath held at 25 ± 0.5 °C and with a Hewlett-Packard memory unit. Output voltage was adjusted to 5 V for zero absorbance. Equal volumes of cacodylate buffered solutions of PIH, PBH, SIH, and SBH (4×10^{-5} to 5×10^{-4} M) and $FeSO_4$ (4×10^{-4} to 2×10^{-3} M) were simultaneously injected into the mixing chamber (mixing time $< 3 \times 10^{-3}$ s). The experimental signals were accumulated at least two times for each experiment.

Signal Analysis. All the signals used were pure exponentials and were analyzed by the semilog and by the Guggenheim methods.[19]

Results

PIH, PBH, SIH, and SBH consist of two different rings, each of which exists in the aqueous medium as several prototropic species.[11,12] Pyridoxal prototropic behavior has been thoroughly analyzed, and this species is known to be present in aqueous media under at least four pH-dependent structures.[11,12] Furthermore, the isonicotinoyl moiety can protonate at the pyridine nitrogen, the salicylaldehyde can deprotonate at the hydroxyl, and finally the amine of the hydrazone bridge can be either deprotonated or protonated. These four synthetic ligands exist, therefore, in aqueous media as several pH-dependent conformations (Chart II). PIH represents the most general case and exists in aqueous media as at least five different pH-dependent structures (Chart

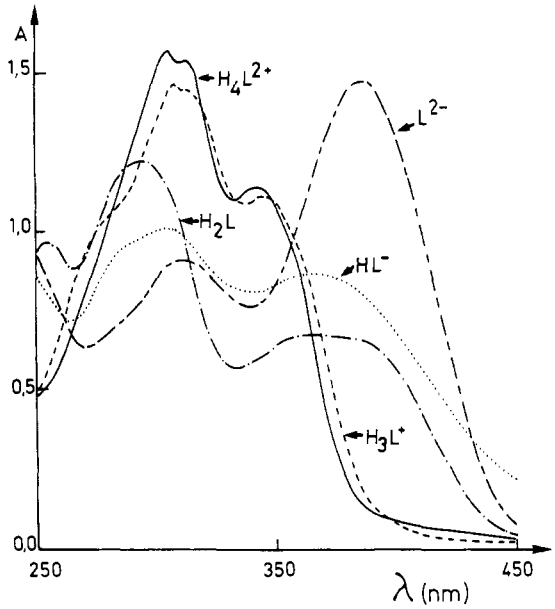

Figure 1. Absorbance spectra of PIH ($c_1 = 1 \times 10^{-4}$ M) at (—) pH = 3.19, (---) pH = 6.60, (···) pH = 10.08, and (-·-) pH = 11.92.

Table I. Prototaumerism pKs of PIH, PBH, SIH, and SBH

compd	pK_1 ± 0.04	pK_2 ● 0.04	pK_3 ± 0.04	pK_4 ± 0.04
PIH	2.26	4.52	7.68	10.10
PBH		4.59	8.47	11.40
SIH		3.33	8.30	11.30
SBH			6.77	

II). Each of the other synthetic ligands would, therefore, correspond to a case described in mechanism I.

mechanism I

$$H_4L^{2+} \rightleftharpoons H_3L^+ + H^+ \qquad K_1 = [H_3L^+][H^+]/[H_4L^{2+}] \quad (1)$$

$$H_3L^+ \rightleftharpoons H_2L + H^+ \qquad K_2 = [H_2L][H^+]/[H_3L^+] \quad (2)$$

$$H_2L \rightleftharpoons HL^- + H^+ \qquad K_3 = [HL^-][H^+]/[H_2L] \quad (3)$$

$$HL^- \rightleftharpoons L^{2-} + H^+ \qquad K_4 = [L^{2-}][H^+]/[HL^-] \quad (4)$$

The facts that each of the structures of Chart II displays a typical absorbance spectrum (Figure 1) and that the differences between the successive pKs of the acid–base reactions involved in mechanism I are sufficiently large allow the use of the Benesi and Hildebrandt relation, which can be expressed for each of these acid–base equilibria as[19]

$$1/\Delta A = 1/\Delta A_f + [H^+]/\Delta A_f K \quad (5)$$

in which $\Delta A = A - A_f$, $\Delta A_f = A_0 - A_f$, A is the absorbance, A_0 is that of the acidic species, A_f is that of the basic species, c_1 is the analytical ligand concentration, and K is the dissociation constant. Linear least-squares regressions of the data against eq 5 for each of the acid–base reactions of mechanism I permit the measurements all the pKs involved in the prototropic transformations of PIH, PBH, SIH, and SBH (Table I). These results show that in the vicinity of neutrality, PIH, PBH, and SIH are present in one major form while PBH exists as the H_2L and HL^- structures. As already mentioned, iron mobilization can occur in endocytic vesicles, the pH of which varies from about 5.5 to neutrality.[13,14] The kinetics were, therefore, performed near neutrality (pH = 6.86).

When Fe(II) (concentration c_2) is mixed with a neutral solution of each of the four ligands (concentration c_1), two c_2-dependent modifications in the 300–500-nm absorbance spectrum of each of the chelates are observed. The first occurs for $c_2 < c_1/2$, and the second is observed with a large excess of Fe(II) ($c_2 \sim 10c_1$). It can, therefore, be assumed that the first spectroscopic modification results mainly from the formation of a complex between

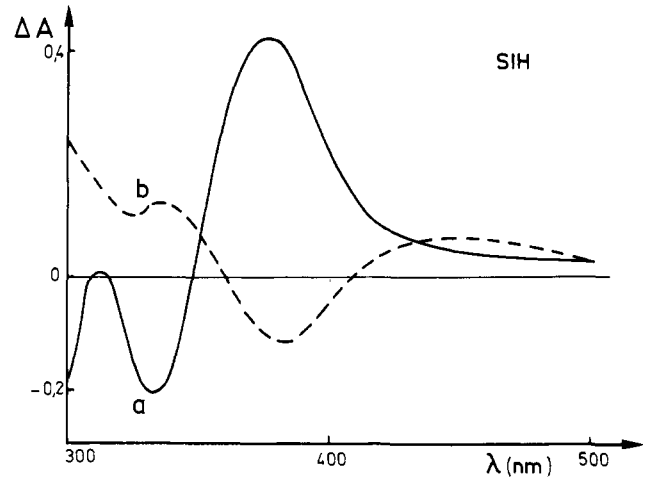

Figure 2. Differential absorbance spectra recorded after a fast stopped-flow mixing of two solutions of SIH and Fe(II) for $c_1 = 10^{-4}$ M and $c_2 = 8 \times 10^{-4}$ M at 25 °C and 0.2 M ionic strength: (a) $\Delta A = A_1 - A_L$, in which A_1 is the absorbance at the end of the fast phenomenon and A_L is the absorbance of the ligand in the absence of iron; (b) $\Delta A = A_f - A_L$, in which A_f is the absorbance at the final state of equilibrium.

Fe(II) and two ligands when there is excess chelating ligand, whereas the second modification is probably due to complexes between Fe(II) and one ligand when there is excess iron. We will, therefore, in a first assumption presume that Fe(II) is complexed by one and two neutral ligands L.

$$Fe^{2+} + H_2L \underset{k_{21}}{\overset{k_{12}}{\rightleftharpoons}} FeH_2L^{2+} \quad (6)$$

$$FeH_2L^{2+} + H_2L \underset{k_{32}}{\overset{k_{23}}{\rightleftharpoons}} Fe(H_2L)_2^{2+} \quad (7)$$

We were not able to measure $K_{c_1} = [Fe^{2+}][H_2L]/[FeH_2L^{2+}]$ and $K_{c_2} = [FeH_2L^{2+}][H_2L]/[Fe(H_2L)_2^{2+}]$ by classical techniques, probably because their values are too close to each other to be determined by conventional spectrophotometric methods.

Kinetic Analysis. When a cacodylate-buffered solution of SIH is mixed in a stopped-flow experiment with a mildly acidic Fe(II) solution, two kinetic phenomena are observed in the 300–500-nm range. The first is a fast exponential modification of absorbance the amplitude of which depends on the wavelength. It is followed by a slower exponential which is also wavelength dependent. The differential absorbance spectrum measured at the end of the fast phenomenon, before the detection of the slow process, and that measured at the final state of equilibrium (Figure 2) led us to chose a wavelength where the amplitude of the fast process is the highest and another where it is negligible as compared to the amplitude of the slower phenomenon (Figure 3). Similar observations were made with PIH, PBH, and SBH. Since all the observed kinetic signals were pure exponentials, they were treated as relaxation modes.[19]

First Relaxation Process. Our kinetic experiments are performed in the direction of complex formation (concentration jump of $[Fe^{2+}]$ and $[H_2L]$) and not in that of complex dissociation (concentration jump of $[FeH_2L^{2+}] - [Fe(H_2L)_2^{2+}]$ and $[H_2L]$). In this case, if the fast phenomenon of Figures 2 and 3 is reaction 7, reaction 6 will be rate-limiting, and reaction 7 will occur constantly during reaction 6. This leads to the observation of a single kinetic phenomenon describing the rate-limiting step.[19] However, two kinetic phenomena are detected for bicomplex formation (Figure 3). We, therefore, ascribe the fast relaxation of Figure 3 to the formation of monocomplex FeH_2L^{2+} (reaction 6) and the second one to the formation of bicomplex $Fe(H_2L)_2^{2+}$. At the end of the fast relaxation and just before the beginning of the second process of Figure 2 (semiequilibrated state), the rate equation of reaction 6 is expressed as

$$-d[FeH_2L^{2+}]/dt = -k_{12}[Fe^{2+}][H_2L] + k_{21}[FeH_2L^{2+}] \quad (8)$$

In the most general case, if it is assumed that neutral species H_2L

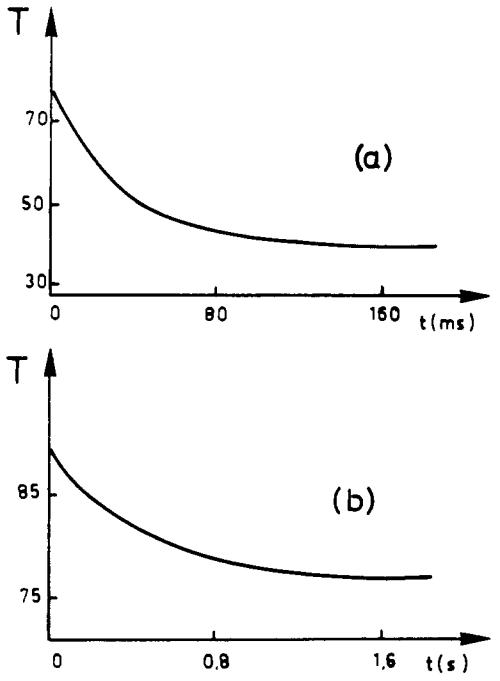

Figure 3. Transmittance change after a fast stopped-flow mixing of two solutions of SIH ($c_1 = 10^{-4}$ M) and Fe(II) ($c_2 = 2 \times 10^{-4}$ M) at 25 °C and 0.2 M ionic strength: (a) at $\lambda = 380$ nm within a time range of 200 ms; (b) at $\lambda = 440$ nm.

Table II. Rate and Stability Constants for Monocomplex FeH_2L Formation from Fe(II) and PIH, PBH, SIH, and SBH

ligand	$10^{-5}k_{12}$, mol^{-1} dm^3 s^{-1}	k_{21}, s^{-1}	$10^5 k_{c_1}$, mol dm^{-3}
PIH	1.65 ± 0.10	2.15 ± 0.20	1.30 ± 0.15
PBH	1.70 ± 0.10	1.75 ± 0.15	1.00 ± 0.10
SIH	0.86 ± 0.05	7.35 ± 0.85	8.50 ± 0.80
SBH	0.61 ± 0.20	6.60 ± 0.62	10.8 ± 0.45

of PIH, PBH, and SIH react with iron to form monocomplex FeH_2L^{2+}, in the vicinity of neutrality the reciprocal relaxation time equation associated with reaction 6 can be expressed as[19]

$$\tau_1^{-1} = k_{12}([Fe^{2+}] + [H_2L]) + k_{21} \quad (9)$$

The approximation of chemical relaxation cannot be applied on such a system, unless $c_2 \geq 2c_1$.[20] Moreover, $[Fe^{2+}]$ and $[FeH_2L^{2+}]$ cannot be directly measured in the reaction medium. They can, however, be determined at the semiequilibrated state from eqs 10 and 11, which are easily derived from the conservation of mass

$$[Fe^{2+}] = c_2 - [FeH_2L^{2+}] \quad (10)$$

$$[H_2L] = c_1 - [FeH_2L^{2+}] \quad (11)$$

$$[FeH_2L^{2+}] = \tfrac{1}{2}\{(c_2 - c_1 + K_{c_1}) + [(c_2 - c_1 + K_{c_1})^2 + 4c_1K_{c_1}]^{1/2}\}$$

and from K_{c_1}. Both equations require the knowledge of the K_{c_1} value. Nevertheless, for $K_{c_1} \leq 10^{-4}$ mol dm^{-3} (which is expected for similar chelating ligands[21-23]) and $c_2 \geq 2c_1$, $[H_2L]$ becomes negligible as compared to $[Fe^{2+}]$. It was, therefore, assumed that $K_{c_1} \leq 10^{-4}$ mol dm^{-3}, and our experiments were performed at $c_2 > 2c_1$. Linear least-squares regressions of the data for PIH, PBH, and SIH in eq 9 gave k_{12}, k_{21}, and K_{c_1} for the three chelating ligands (Figure 4, Table II). In this analysis, it was assumed that iron reacted with the neutral species of each of the four

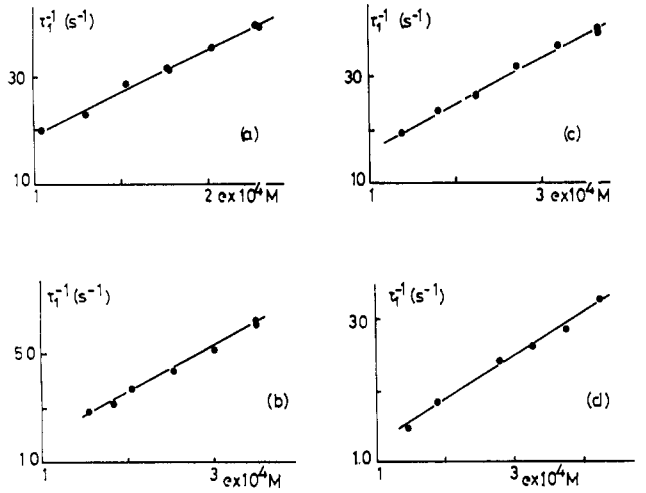

Figure 4. Plot of $\epsilon = [Fe^{2+}] + [H_2L]$ against τ_1^{-1} for the following: (a) PIH, intercept 2.15 ± 0.20 s^{-1}, slope (1.65 ± 0.10) × 10^5 mol^{-1} dm^3 s^{-1}, $r = 0.9967$; (b) PBH, intercept 1.75 ± 0.15 s^{-1}, slope (1.70 ± 0.10) × 10^5 mol^{-1} dm^3 s^{-1}, $r = 0.9964$; (c) SIH, intercept 7.35 ± 0.85 s^{-1}, slope (8.5 ± 0.50) × 10^4 mol^{-1} dm^3 s^{-1}, $r = 0.9949$; (d) SBH, intercept 6.60 ± 0.62 s^{-1}, slope (0.60 ± 0.06) × 10^5 mol^{-1} dm^3 s^{-1}, $r = 0.9962$.

synthetic chelating ligands. However, iron can react with either the acidic species of the chelating ligand H_3L^+ and/or the basic species HL^- (reactions 12 and 13). Reciprocal relaxation time

$$Fe^{2+} + H_3L^+ \underset{k'_{21}}{\overset{k'_{12}}{\rightleftharpoons}} FeH_3L^{3+} \quad (12)$$

$$K'_{c_1} = [Fe^{2+}][H_3L^+]/[FeH_3L^{3+}]$$

$$Fe^{2+} + HL^- \underset{k''_{21}}{\overset{k''_{12}}{\rightleftharpoons}} FeHL^+ \quad (13)$$

$$K''_{c_1} = [Fe^{2+}][HL^-]/[FeHL^+]$$

eqs 14 and 15 can be associated with reactions 12 and 13, respectively.[18,19]

$$\tau'^{-1} = k'_{12}[Fe^{2+}][H^+]/([H^+] + K_2) + k'_{21} \quad (14)$$

$$\tau''^{-1} = k''_{12}[Fe^{2+}]K_3/([H^+] + K_3) + k''_{21} \quad (15)$$

In both cases the slopes of regression lines a–c of Figure 4 (the k_{12} values reported in Table II) lead under our experimental conditions (pH = 6.86) to k'_{12} and k''_{12} values in the 10^8–10^9 mol^{-1} dm^3 s^{-1} range, which is much too high as compared with second-order rates for first complex formation with iron.[21,22] Therefore, complex formation occurs between Fe^{2+} and the neutral species of PIH, PBH, and SIH with rates similar to those reported in the literature.[21,22] However, under our experimental conditions, SBH exists as two species, H_2L and HL^-, both of which can react with iron to form a complex (reactions 6 and 13). Reciprocal relaxation time equations associated with these two reactions are eqs 16 and 15, respectively.[18,19]

$$\tau^{-1}{}_1 = k_{12}[Fe^{2+}][H^+]/([H^+] + K_3) + k_{21} \quad (16)$$

The use these two equations does not permit to precise the nature of the PBH species involved in complex formation because, at pH = 6.86, $K_3([H^+] + K_3) \sim [H^+]/([H^+] + K_3)$. Therefore, the slope of the line of Figure 4c (6.0×10^4 mol^{-1} dm^3 s^{-1}) is probably the average rate for complex formation of the H_2L and/or the HL^- species of SBH with Fe^{2+}.

Second Relaxation Process. Reaction 6 is faster than reaction 7. It is, therefore, assumed that reaction 6 is constantly equilibrated during reaction 7. This allows the use of chemical relaxation formalism[18,19] to derive the equation of the reciprocal

(20) (a) Brouillard, R. *J. Chem. Soc., Faraday Trans. 1* **1980**, *76*, 583. (b) Bertigny, J. P.; Dubois, J. E.; Brouillard, R. *Ibid.* **1983**, *79*, 209.
(21) Eigen, M.; Wilkins, R. G. *Adv. Chem. Ser.* **1965**, *No. 49*, 55.
(22) Hague, D. N. *Chemical Relaxation in Molecular Biology*; Pecht, I., Rigler, R., Eds.; Springer-Verlag: Berlin, 1977; pp 84–106.
(23) Hancock, R. D.; Martell, A. E. *Chem. Rev.* **1989**, *89*, 1875.

Table III. Rate and Stability Constants for the Formation of Bicomplex FeL_2 from Monocomplex FeL for PIH, PBH, SIH, and SBH

ligand	$10^{-4}k_{23}$, mol^{-1} dm^3 s^{-1}	k_{32}, s^{-1}	$10^5K_{c_2}$, mol dm^{-3}
PIH	2.45 ± 0.15	0.25 ± 0.05	1.00 ± 0.09
PBH	3.05 ± 0.15	0.25 ± 0.03	0.80 ± 0.07
PIH	4.00 ± 0.25	0.80 ± 0.07	2.00 ± 0.20
SBH	1.5 ± 0.10	0.60 ± 0.06	4.00 ± 0.20

relaxation time associated with reaction 7 whose rate equation can be expressed as

$$-d[Fe(H_2L)_2^{2+}]/dt = -k_{23}[FeH_2L^{2+}][H_2L] + k_{32}[Fe(H_2L)_2^{2+}] \quad (17)$$

Conservation of mass implies

$$\Delta[H_2L] + \Delta[FeH_2L^{2+}] + 2\Delta[Fe(H_2L)_2^{2+}] = 0 \quad (18)$$

$$\Delta[FeH_2L^{2+}] + \Delta[Fe(H_2L)_2^{2+}] + \Delta[Fe^{2+}] = 0 \quad (19)$$

Since reactions 6 and 3 are in a constant state of equilibrium during reaction 7, we can write

$$\Delta[FeH_2L^{2+}] = [H_2L](\Delta[Fe^{2+}])/K_{c_1} + [Fe^{2+}](\Delta[H_2L])/K_{c_1} \quad (20)$$

$$\Delta[H_2L] = [H^+](\Delta[HL^-])/K_2 + [HL^-](\Delta[H^+])/K_2 \quad (21)$$

From eqs 17–21, we can deduce the reciprocal relaxation time equation associated with reaction 7 in neutral buffered media.

$$\tau_2^{-1} = k_{23}\delta + k_{32} \quad (22)$$

Here $\delta = (2[Fe^{2+}] + [H_2L])[H_2L]/\gamma + (2K_{c_1} + [H_2L])\cdot[FeH_2L^{2+}]/\gamma$, with $\gamma = K_{c_1} + [Fe^{2+}] + [H_2L]$.

$[FeH_2L^{2+}]$ and $[H_2L]$ cannot be measured directly. The fact that in our experimental conditions $c_1 > c_2$ leads to $[Fe^{2+}] > [H_2L]$. This, moreover, allows us to assume to a first approximation that $[FeH_2L^{2+}] > [Fe(H_2L)_2^{2+}]$ and $[H_2L]$. A linear least-squares regression of the data with the simplified rate eq 23 gives a first approximation to the elementary rate constants

$$\tau_2^{-1} = 2k_{23}c_1K_{c_1}/(K_{c_1} + c_2 - c_1) + k_{32} \quad (23)$$

k_{23} and k_{32} and complex formation constant K_{c_2}. Knowing K_{c_1}, given an approximation to K_{c_2}, and given that at the final equilibrated state

$$c_1 = [H_2L] + [FeH_2L^{2+}] + 2[Fe(H_2L)_2^{2+}] \quad (24)$$

$$c_2 = [Fe^{2+}] + [FeH_2L^{2+}] + [Fe(H_2L)_2^{2+}] \quad (25)$$

we can derive eqs 26–28, where $X = [H_2L]^2 + K_{c_2}[H_2L] + K_{c_1}K_{c_2}$.

$$[Fe(H_2L)_2^{2+}] = [H_2L]^2c_2/X \quad (26)$$

$$[FeH_2L^{2+}] = c_2K_{c_2}[H_2L]/X \quad (27)$$

$$[Fe^{2+}] = c_2K_{c_1}K_{c_2}/X \quad (28)$$

From eqs 24–28, considering the fact that under our experimental conditions $[H_2L] \ll [Fe^{2+}]$, we can derive eq 29.

$$[H_2L] = \{[(c_2/K_{c_1})^2 + (8c_1c_2/K_{c_1}K_{c_2})]^{1/2} - c_2/K_{c_1}\}K_{c_1}K_{c_2}/4c_2 \quad (29)$$

From eqs 26–29, we can deduce approximations to δ. A new linear least-squares regression of these estimates against τ_2^{-1} gives new values of k_{23}, k_{32}, and K_{c_2}, which allows a new δ to be measured. This cycle is repeated until ΔK_{c_2} (the difference between the K_{c_2} estimate and that measured from the new regression line) is a minimum. This corresponds to the best regression line achieved with our experimental data and, therefore, gives the best possible k_{23}, k_{32}, and K_{c_2} (Figure 5, Table III). However, in the case of SBH, bicomplex formation can occur with HL^- and/or H_2L, which lead us to regard the slope of the line of Figure 5d as the average second-order rate constant of bicomplex formation with Fe^{2+}.

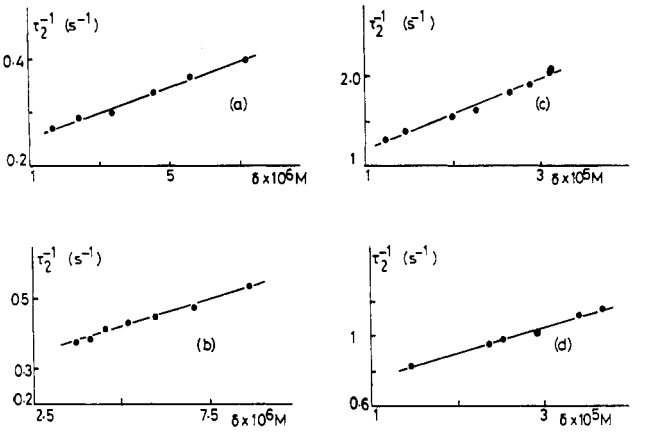

Figure 5. Plot of δ against τ_2^{-1} for the following: (a) PIH, intercept 0.25 ± 0.05 s^{-1}, slope (2.45 ± 0.15) × 10^4 mol^{-1} dm^3 s^{-1}, r = 0.9937; (b) PBH, intercept 0.25 ± 0.03 s^{-1}, slope (3.05 ± 0.15) × 10^4 mol^{-1} dm^3 s^{-1}, r = 0.9946; (c) SIH, intercept 0.80 ± 0.07 s^{-1}, slope (4.00 ± 0.25) × 10^4 mol^{-1} dm^3 s^{-1}; r = 0.99220; (d) SBH, intercept 0.60 ± 0.06 s^{-1}, slope (1.50 ± 0.10) × 10^4 mol^{-1} dm^3 s^{-1}, r = 0.9956.

Absorbance Spectra of FeH_2L^{2+} and $Fe(H_2L)_2^{2+}$ for PIH, PBH, SIH, and SBH. When a solution of H_2L is rapidly mixed with Fe(II), we observe the two relaxation processes already reported in Figure 3. If $c_1 > c_2$, because reaction 6 is much faster than reaction 7, at the end of the first phenomenon and before the beginning of the second relaxation, c_1 is totally transformed into FeH_2L^{2+}. At this precise moment, the absorbance spectrum would be due to FeH_2L^{2+} and Fe^{2+} only (Figure 2), and at the final equilibrated state (after the end of the slow phenomenon of Figure 3), the absorbance is due to H_2L, Fe^{2+}, FeH_2L^{2+}, and $Fe(H_2L)_2^{2+}$. Above 300 nm the contribution of Fe^{2+} to this absorbance is negligible, which allows the absorbance to be expressed according to the Beer–Lambert law as

$$A = (\epsilon_1[H_2L] + \epsilon_2[FeH_2L^{2+}] + \epsilon_3[Fe(H_2L)_2^{2+}])l \quad (30)$$

in which ϵ_1, ϵ_2, and ϵ_3 are the molecular absorbance coefficients of H_2L, FeH_2L^{2+}, and $Fe(H_2L)_2^{2+}$, respectively, and l is the optical path, which in our case is 1 cm. Equation 30 can also be written as

$$(A - \epsilon_1[H_2L] - \epsilon_2[FeH_2L^{2+}])/[Fe(H_2L)_2^{2+}] = \epsilon_3 \quad (31)$$

$[H_2L]$, $[FeH_2L^{2+}]$, and $[Fe(H_2L)_2^{2+}]$ can be deduced from eqs 26–29. Equation 31 allows, therefore, the determination of ϵ_3 at any wavelength. This permits the absorbance spectrum of $Fe(H_2L)_2^{2+}$ to be measured (Figure 6).

Discussion

It is accepted that complex formation occurs preferentially with the metal ion which has the highest degree of oxidation.[22,23] This rule is not, however, restrictive, and with ligands such as phenanthroline, dipyridyl, R–N=C, etc., complex formation occurs mostly with low-valency metal ions.[23] Therefore, in the case of PIH, PBH, SIH, and SBH, the nitrogen of the hydrazone bridge would favor complex formation with Fe(II), while the two oxygens of the phenolate and of the carbonyl would form a more stable complex with Fe(III).[22,23] On the other hand, ligands with high affinity for Fe(III) enhance the oxidation of Fe(II),[10] which can be detected as an apparent modification of the redox potential of the metal ion in the complex.[24] This can explain the finding that even when complex formation occurs with Fe(II), the latter is detected as oxidized to Fe(III) in the final product.[9] Oxidation of Fe(II) in the complex by atmospheric oxygen, for example, is much slower than complex formation.[10] However, in order to avoid it, our experiments were performed under argon in oxygen-free media and in the absence of any reducible species. In addition, the kinetic analysis, which led us to propose a two-step mechanism

(24) Ibanez, J. G.; Gonzalez, I.; Gardena, M. A. *J. Chem. Educ.* **1988**, *65*, 173.

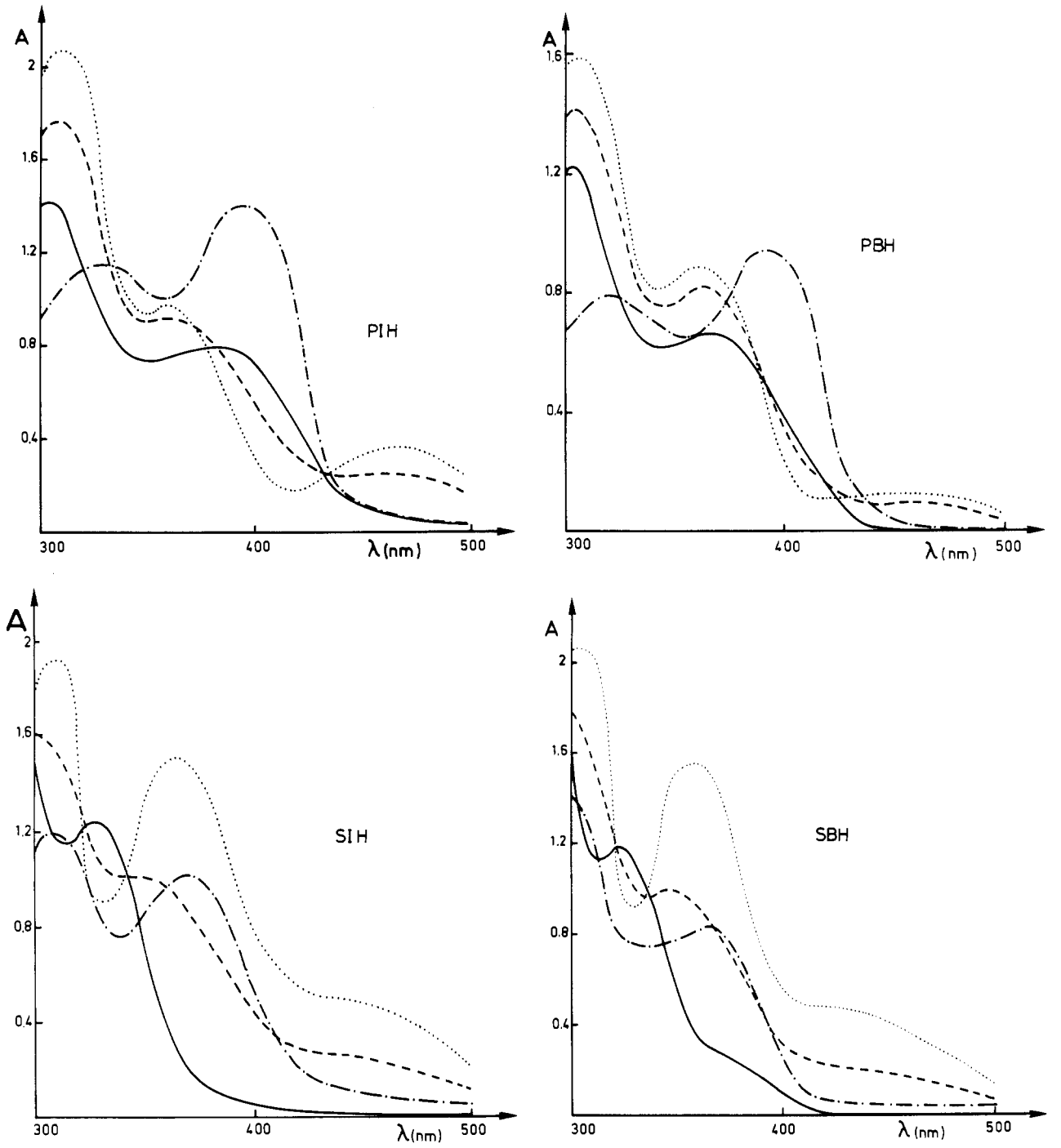

Figure 6. Absorbance spectra at pH 6.86 of 10^{-4} M of the H_2L (—), FeH_2L^{2+} (-·-), and $Fe(H_2L)_2^{2+}$ (···) species of PIH, PBH, SIH, and SBH as compared to the spectrum (- - -) measured at the final state of equilibrium for $c_1 = 1 \times 10^{-4}$ M and $c_2 = 0.5 \times 10^{-4}$ M at 25 °C and 0.2 M ionic strength. The FeH_2L^{2+} spectra are measured at the semiequilibrated state just before the formation of $Fe(H_2L)_2^{2+}$ after a fast $[Fe^{2+}] + [H_2L]$ mixing, while the spectra of $Fe(H_2L)_2^{2+}$ are calculated by the use of eq 31.

on the basis of the observation of only two relaxation modes, would not have been possible if oxidation was occurring during complex formation. Finally, the second-order rate constants measured for complex formation with PIH, PBH, SIH, and SBH (Tables II and III) are typically those reported for Fe(II) (about 10^4–10^6 mol dm^{-3} s^{-1})[22] and cannot be ascribed to complex formation with Fe(III) (second-order rates of about 50–10^3 mol^{-1} dm^3 s^{-1}).[22] We can, therefore, safely state that our kinetic and thermodynamic analysis concerns only Fe(II) complexes.

Complex Stabilities. In Table IV, we report the stability constants of bicomplexes of PIH, PBH, SIH, and SBH with Fe(II). X-ray and IR analyses seem to indicate that, in the crystal of the PIH–Fe(III) complex, the ligands are in a tridentate conformation where phenol and hydrazide protons are transferred to the pyridine nitrogen atoms on the pyridoxal and the isonicotinoyl rings.[7,8] Therefore, these latter are both in a zwitterionic form (Chart III). However, in aqueous media and in the absence of a metal ion, if the hydrazide proton transfer to the pyridine nitrogen of isonicotinoyl were to occur, the related zwitterion (Chart III) would have a stability range in the pH 6 region (between the deprotonation pK of the hydrazone (pK_4 = 10.1,

Table IV. Affinity Constants for Complex Formation from Fe(II) and 2 equiv of PIH, PBH, SIH, and SBH

ligand	$10^5K_{c_1}$, mol dm^{-3}	$10^5K_{c_2}$, mol dm^{-3}	$10^{-9}(1/K_{c_2}K_{c_1})$, mol^{-2} dm^6
PIH	1.30	1.00	7.7 ± 1.2
PBH	1.00	0.80	12.5 ± 1.5
SIH	8.50	2.00	0.60 ± 0.10
SBH	10.80	4.00	0.25 ± 0.05

Chart III

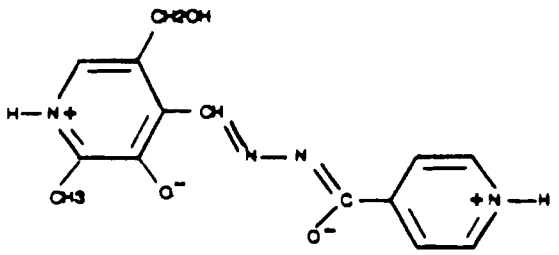

reaction 4, Table I) and that of the pyridinium (pK_1 = 2.26, reaction 1, Table I)). This is quite unlikely, because of the large difference between pK_4 and pK_1 (about 8). Additionally, in PBH, the isonicotinoyl is replaced by a benzoyl, which prevents the hydrazide–pyridine prototautomerism and would, therefore, lead to a less stable complex with iron. Nonetheless, affinity constants of PIH and PBH for Fe(II) are of the same order of magnitude (Table IV). This indicates that with Fe(II), in both complexes, PIH and PBH have a similar tridentate configuration which excludes the existence of a hydrazide–pyridine zwitterion in the Fe(II)–PIH complex. Therefore, the isonicotinoyl is probably engaged in the $Fe^{II}(PIH)_2$ complex in a neutral nonzwitterionic configuration. This analysis does not apply to SIH for which the difference between the pK of pyridine protonation (pK_3 = 3.33, Table I) and that of phenolate protonation (pK_4 = 8.30) is about 5. This can lead to a zwitterion with a stability range in the pH 6 region and which can be involved in complex formation. This zwitterion cannot, of course, occur with SBH, which can explain the lower affinity of the latter for iron as compared to that of SIH (Table IV). As for the pyridoxal moiety in neutral aqueous media, it is zwitterionic[11,12] and is probably directly involved in the Fe(II) and Fe(III) complexes with PIH and PBH. This can also explain the higher stabilities of these complexes as compared to those of SIH and SBH.

Affinity of PIH, PBH, SIH, and SBH for Fe(II) and Efficiency in Its Mobilization. Concluding Remarks. Iron is usually transported into the cell by the interaction of transferrin with a specific receptor situated in the plasma membrane and by the formation of a lipid vesicle containing both receptor and transferrin which is internalized in the cell.[13,14] After internalization of $(Fe^{3+})_2$–transferrin, iron is released within acidic vesicles, and the iron-depleted protein is recycled back to the plasma membrane.[13,14] It is strongly supported that iron mobilization from transferrin occurs according to four sequential steps: (1) acidification of the Fe^{III}_2–transferrin-containing endocytic vesicles; (2) enzymic reduction of Fe(III) to Fe(II); (3) movement of Fe(II) through the membrane by a concentration gradient process; (4) chelation of Fe(II) by cytoplasmic carriers.[14] Ponka et al. also estimated that Fe(III) is reduced before complex formation with PIH and that the removal of the complex from the cell is a very slow process which probably limits the efficiency of the chelate in iron mobilization.[2] However, in view of the complexity of the living cell, and even if iron is reduced into Fe(II) prior to complex formation and removal, we cannot expect a direct correlation between the ability of the chelating ligands to mobilize iron in vivo[6] and their affinity for Fe(II) (Table IV). In this process affinity is one factor among others which need to be investigated further, mostly from a biological standpoint.

Acknowledgment. We are grateful to Drs. J. Lomas and P. Fellman for constructive discussions and to Professors P. Ponka and H. M. Schulman for providing us with the chelating ligands.

Registry No. PIH, 737-86-0; PBH, 72343-06-7; SIH, 495-84-1; SBH, 3232-37-9; Fe, 7439-89-6.

Contribution from the Departments of Chemistry, State University of New York at Buffalo, Buffalo, New York 14214, and State University of New York, College at Fredonia, Fredonia, New York, 14603

Characterization of Protonated *trans*-Bis(dioxime)ruthenium Complexes: Crystal Structures of *trans*-$Ru(DPGH)_2(NO)Cl$, *trans*-$[Ru(DMGH)(DMGH_2)(NO)Cl]Cl$, and *trans*-$Ru(DMGH)_2(NO)Cl$

Lisa F. Szczepura,† James G. Muller,† Carol A. Bessel,† Ronald F. See,† Thomas S. Janik,‡ Melvyn Rowen Churchill,*,† and Kenneth J. Takeuchi*,†

Received November 8, 1991

Single-crystal X-ray diffraction studies were carried out on *trans*-$Ru(DPGH)_2(NO)Cl$ (**1**), *trans*-$[Ru(DMGH)(DMGH_2)(NO)Cl]Cl$ (**2**), and *trans*-$Ru(DMGH)_2(NO)Cl$ (**3**) (DMGH = dimethylglyoxime monoanion, DPGH = diphenylglyoxime monoanion). These represent the first crystal structures of *trans*-bis(dioxime) complexes containing ruthenium. Complex **1** crystallizes in the monoclinic space group $C2/c$, with a = 10.459 (5) Å, b = 10.148 (4) Å, c = 26.673 (13) Å, β = 98.25 (4) Å, Z = 4, V = 2802 (2) Å^3, and R = 4.83%. Complex **2** crystallizes in the monoclinic space group $P2_1/c$, with a = 13.8100 (10) Å, b = 10.095 (2) Å, c = 11.898 (2) Å, β = 100.780 (10) Å, Z = 4, V = 1629.4 (4) Å^3, and R = 3.05%. Complex **3** crystallizes in the orthorhombic space group $P2_12_12_1$, with a = 7.9920 (10) Å, b = 14.251 (2) Å, c = 24.666 (2) Å, Z = 8, V = 2809.1 (5) Å^3, and R = 3.84%. The crystal structure determinations include the location and refinement of hydrogen atoms associated with the oxime oxygens. The existence of two types of hydrogen bonds (O–H--Cl hydrogen bonds and a symmetric O–H--O oxime bridge) associated with the oxime oxygen atoms of *trans*-$[Ru(DMGH)(DMGH_2)(NO)Cl]Cl$ can be clearly demonstrated. Furthermore, the crystal structures of both *trans*-$Ru(DPGH)_2(NO)Cl$ and *trans*-$Ru(DMGH)_2(NO)Cl$ display a third type of hydrogen bonding (asymmetric O–H--O oxime bridge) involving the oxime oxygen atoms. Thus, three types of hydrogen bonding that were previously proposed for *trans*-bis(dioxime) transition metal complexes can be directly observed within these three structurally similar bis(dioxime)ruthenium complexes. In addition, we can now unambiguously assign the O–H stretching IR bands to the proper modes of hydrogen bridging. Temperature-dependent ^1H NMR spectroscopy of *trans*-$[Ru(DMGH)(DMGH_2)(NO)Cl]Cl$ was used to measure rate constants of proton exchange, which demonstrated that the solid-state structure is maintained in solution. Finally, the cyclic voltammograms of complexes **2** and **3** and the pK_a values for the stepwise removal of two protons from complex **2** were measured.

Introduction

The coordination chemistry of *trans*-bis(dioxime) transition metal complexes continues to attract considerable attention as models of vitamin B_{12},[1] dioxygen carriers,[2] halogen atom abstraction agents[3] and catalysts in chemical processes.[4,5] In ad-

†State University of New York at Buffalo.
‡State University of New York, College at Fredonia.

(1) Pahor, N. B.; Dreos-Garlatti, R.; Geremia, S.; Randaccio, L.; Tauzher, G.; Zangrando, E. *Inorg. Chem.* **1990**, *29*, 3437-3441.
(2) Lance, K. A.; Goldsby, K. A.; Busch, D. H. *Inorg. Chem.* **1990**, *29*, 4537-4544.

0020-1669/92/1331-0859$03.00/0